Structure and Properties of Anion-Radical Salt of 7,7,8,8-Tetracyanoquinodimethane with N-Methyl-2,2'-dipyridyl Cation

T. N. Starodub[a,*], D. Fenske[b,c,d], O. Fuhr[c,d], S. Miskiewicz[a], O. N. Kazheva[e], and V. A. Starodub[a†]

[a] Institute of Chemistry, Jan Kochanowski University, Kielce, 25-405 Poland
[b] Institute of Inorganic Chemistry, Karlsruhe Institute of Technology, Karlsruhe, 76131 Germany

[c] Institute of Nanotechnology (INT) and Karlsruhe Nano Micro Facility (KNMF), Karlsruhe Institute of Technology (KIT), Eggenstein-Leopoldshafen 76344, Germany

[d] Lehn-Institute for Functional Materials, School of Chemistry and Chemical Engineering, Sun Yat-Sen University, Guangzhou, 510275 China

[e] Institute of Problems of Chemical Physics, Russian Academy of Sciences, Chernogolovka, Moscow oblast, 142432 Russia
*e-mail: tstarodub@ujk.edu.pl

Abstract—Anion-radical salt of 7,7,8,8-tetracyanoquinodimethane with N-methyl-2,2'-dipyridyl cation is synthesized. Its composition is determined using electron spectroscopy and elemental analysis. The crystal and molecular structures of the salt are determined using X-ray diffraction (XRD) analysis. The salt contains homogeneous stacks of 7,7,8,8-tetracyanoquinodimethane particles, which is a necessary condition for high electrical conductivity. The IR spectrum of the salt exhibits specific features characteristic of organic metals: continuous absorption (electron continuum) and manifestation of electron–phonon interaction. These characteristics of the salt give grounds to assign it to organic metals.

INTRODUCTION

Anion-radical salts (ARSs) based on 7,7,8,8-tetracyanoquinodimethane (TCNQ) have been of great interest since the 1960s, when the first organic TCNQ-based metals were obtained [1, 2]. After the discovery of organic metals and then superconductors based on cation-radical salts [2], the interest to the TCNQ ARSs decreased; however, it arose again in the second half of the 1980s and has not weakened since that time. This fact is primarily due to the discovery of hot melting organic conductors on their basis.

Studies of the magnetic properties of TCNQ ARSs led to the discovery of magnetically ordered ferro- and antiferromagnetic structures [3, 4]. The use of organic cations containing more than one donor atom as counter ions resulted in the dicovery of quasi-two-dimensional organic ARS-based conductors [5]. The presence of nonquaternized donor atoms in the cation composition allows for indirect magnetic exchange between the spins of anion radicals of the neighboring stacks, which was demonstrated by an example of TCNQ ARSs with pyrazine-based cations [6 8].

These investigations were continued on a TCNQ-based ARS with N-methyl-2,2'-dipyridyl cation, described by the formula
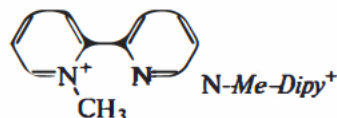
Complexes of 2,2'-dipyridyl exhibit antioxidant, antibacterial, and antifungal properties [9]. Based on *Dipy*, one can construct efficient biosensors for detecting pathogenic flora in food [10]. Therefore, TCNQ ARSs with *Dipy*-based cations can be used in biotechnology.

In this paper, we report the preparation of ARS (N–*Me*–*Dipy*)(TCNQ)$_2$ (**1**) single crystals, describe their crystal and molecular structures, and present data obtained based on their IR spectra.

EXPERIMENTAL

7,7,8,8-Tetracyanoquinodimethane, 2,2'-dipyridyl, methyl chloride, and lithium iodide (Aldrich) were used without additional purification. LiTCNQ salt was synthesized in acetonitrile, and the dipyridyl

† Deceased.

Table 1. Bond distances in structure **1**

Bond	Length, Å	Bond	Length, Å
N1–C1	1.367(5)	C27–C33	1.404(5)
N1–C5	1.363(4)	C28–C29	1.356(4)
N1–C11	1.490(5)	C30–C31	1.430(6)
N2–C6	1.356(4)	C30–C32	1.424(6)
N2–C10	1.338(5)	C33–C34	1.420(6)
C1–C2	1.358(5)	C33–C35	1.421(5)
C2–C3	1.374(6)	N3–C19	1.142(5)
C3–C4	1.373(5)	N4–C20	1.146(5)
C4–C5	1.381(5)	N5–C22	1.154(5)
C5–C6	1.483(5)	N6–C23	1.139(5)
C6–C7	1.383(5)	C12–C13	1.445(5)
C7–C8	1.381(5)	C12–C17	1.439(5)
C8–C9	1.367(6)	C12–C18	1.390(5)
C9–C10	1.379(5)	C13–C14	1.347(5)
N7–C31	1.142(5)	C14–C15	1.438(5)
N8–C32	1.150(5)	C15–C16	1.435(5)
N9–C34	1.149(5)	C15–C21	1.389(5)
N10–C35	1.150(5)	C16–C17	1.345(4)
C24–C25	1.435(5)	C18–C19	1.436(6)
C24–C29	1.429(5)	C18–C20	1.436(6)
C24–C30	1.398(5)	C21–C22	1.427(6)
C25–C26	1.350(5)	C21–C23	1.431(5)
C26–C27	1.431(5)	N11–C36	1.138(6)
C27–C28	1.425(5)	C36–C37	1.450(6)

Table 2. Bond angles in structure **1**

Bond	Angle, deg	Bond	Angle, deg
C1–N1–C11	116.3(3)	C32–C30–C31	117.04(3)
C5–N1–C1	120.7(3)	N7–C31–C30	178.3(5)
C5–N1–C11	123.0(3)	N8–C32–C30	178.6(5)
C10–N2–C6	116.3(4)	C27–C33–C34	122.0(4)
C2–C1–N1	120.6(4)	C27–C33–C35	122.6(4)
C1–C2–C3	120.1(4)	C34–C33–C35	115.3(3)
C4–C3–C2	118.7(4)	N9–C34–C33	178.5(5)
C3–C4–C5	121.5(3)	N10–C35–C33	177.7(5)
N1–C5–C4	118.3(3)	C17–C12–C13	117.6(3)
N1–C5–C6	122.1(3)	C18–C12–C13	120.9(3)
C4–C5–C6	119.6(3)	C18–C12–C17	121.4(3)
N2–C6–C5	112.9(3)	C14–C13–C12	120.9(3)
N2–C6–C7	122.8(3)	C13–C14–C15	121.2(3)
C7–C6–C5	124.0(3)	C16–C15–C14	117.9(3)
C8–C7–C6	118.8(4)	C21–C15–C14	120.9(3)
C9–C8–C7	119.5(4)	C21–C15–16	121.2(3)
C8–C9–C10	118.2(4)	C17–C16–C15	121.2(3)
N2–C10–C9	124.4(4)	C16–C17–C12	121.2(3)
C29–C24–C25	117.4(3)	C12–C18–C19	121.9(4)
C30–C24–C25	121.2(4)	C12–C18–C20	121.6(4)
C30–C24–C29	121.4(3)	C19–C18–C20	116.5(3)
C26–C25–C24	121.2(3)	N3–C19–C18	179.3(4)
C25–C26–C27	121.3(3)	N4–C20–C18	179.6(5)
C28–C27–C26	117.6(3)	C15–C21–C22	122.4(4)
C33–C27–C26	121.1(3)	C15–C21–C23	123.0(3)
C33–C27–C28	121.3(3)	C22–C21–C23	114.6(3)
C29–C28–C27	121.3(3)	N5–C22–C21	177.4(4)
C28–C29–C24	121.2(3)	N6–C23–C21	177.3(4)
C24–C30–C31	121.6(4)	N11–C36–C37	178.7(6)
C24–C30–C32	121.4(4)		

quaternization reaction was also performed in acetonitrile.

ARS was synthesized according to the following reaction:

$$\text{N-}Me\text{-}Dipy^{+}Br^{-} + LiTCNQ + TCNQ$$

$$\rightarrow (\text{N-}Me\text{-}Dipy)(TCNQ)_2\downarrow + LiBr.$$
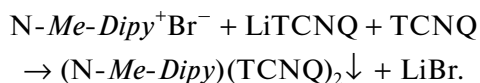
Crystals **1** were filtered, washed with diethyl ether, and dried in air. The ARS composition was found using the spectrophotometric technique described in [11] and confirmed by elemental analysis. The found contents are as follows: C 71.53, H 3.74 and N 24.91 wt %. The chemical formula is $C_{37}H_{22}N_{11}$. The calculated contents are C 71.60, H 3.57 and N 24.82 wt %.

The structure of the synthesized ARS was determined on a Stoe StadiVari diffractometer. The measurements were performed at a temperature of 140.15 K. The structure was solved using the Olex2 [12] and ShelXT [13] software. Refinement was performed by the least-squares method in the ShelXL program [13].

The main crystallographic parameters of $C_{37}H_{22}N_{11}$ (M = 620.65 g/mol) are as follows: orthorhombic sp. gr. $P2_12_12_1$ (no. 19), a = 7.5644(4) Å, b = 12.7028(7) Å, c = 31.7026(15) Å, V = 3046.3(3) Å³, Z = 4, μ(GaK_{α}) = 0.442 mm⁻¹, D_{calc} = 1.353 g/cm³, 20772 measured reflections (6.522° ≤ 2θ ≤ 119.978°) and 6779 independent reflections (R_{int} = 0.0514, R_{sigma} = 0.0790), which were used in all calculations. The final values were R_1 = 0.0477 ($I > 2\sigma(I)$) and wR_2 = 0.1272 (based on all data).

The values of bond lengths and bond angles are listed in Tables 1 and 2, respectively, and Fig. 1 shows the structure of compound **1** with enumerated atoms. The crystallographic data have been deposited to the Cambridge Crystallographic Data Centre (CCDC no. 2006758) and can be accessed at www.ccdc.cam.uk.conts/retrieving (CCDC, 12 Union Road, Cambridge CB21 EZ, the United Kingdom; fax: +44 1223 336 033; deposit@ccdc.cam.ac.uk).
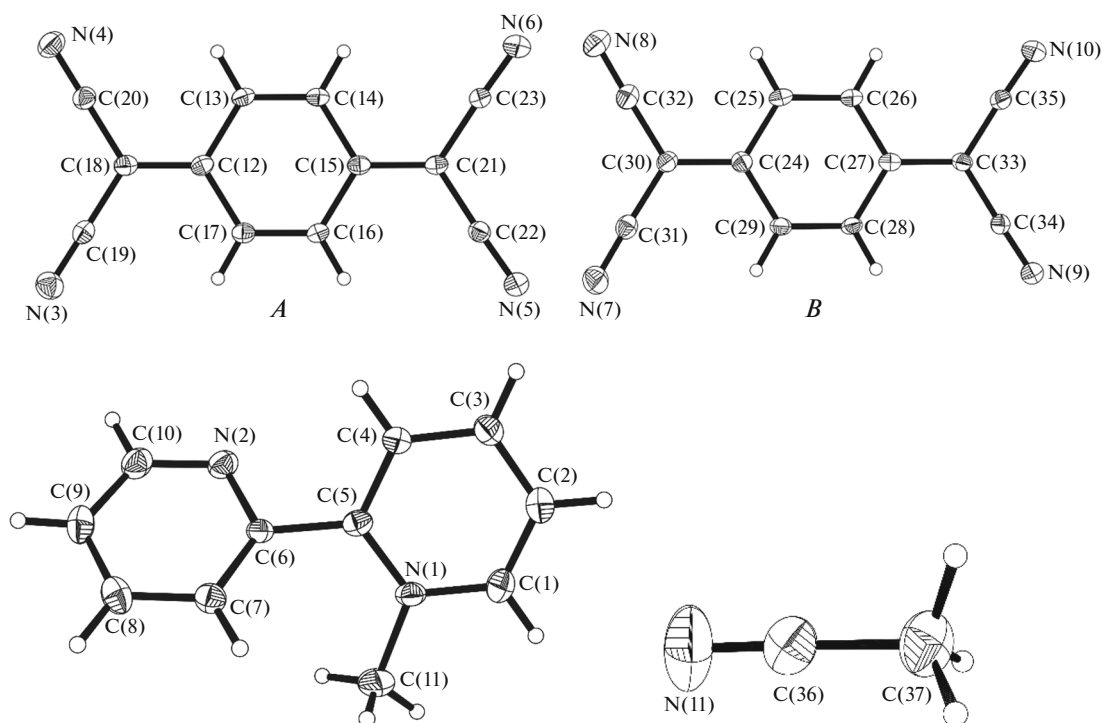
Fig. 1. Structure of anion-radicals (*A* and *B*), a cation, and an acetonitrile molecule in structure **1** (ellipsoids are drawn at the 30% probability level).

IR spectra were recorded on a Nicoletis 10 spectrophotometer (Thermo Scientific) with a SmartMIRacle attachment in the wavelength range of $600-4000$ cm^{-1}. Figure 2 shows the IR spectrum of salt **1**.

RESULTS AND DISCUSSION

The crystal structure of ARS **1** is formed by two TCNQ$^{-\bullet}$ anion-radicals (A and B), a N-methyl-2,2'-dipyridyl cation, and a solvent molecule, which are located in the general sites of unit cell (Fig. 3). The cation geometry deviates from the planar one, which is apparently due to the steric effect of the methyl group (the dihedral angle between the planes of *N*-cycles is 41.3°). TCNQ$^{-\bullet}$ anion-radicals are characterized by a planar structure: the maximum deviations of all atoms (except for hydrogen atoms) from their averaged planes do not exceed 0.06 and 0.03 Å for atoms *N*(3) and *N*(9), respectively. The salt is characterized by a layered crystal structure, in which the layers formed by cations and solvent molecules alternate with the layers of TCNQ$^{-\bullet}$ anion-radicals in the direction along the *c* axis (Fig. 3). Anion-radicals form stacks (Fig. 4), in which *A...B...A...B* sequences alternate. The distance between the averaged planes of anion radicals in a stack is 3.19 Å, and the dihedral angles between these planes are 179.9°. The neighboring stacks in a layer are shifted along the long axis of the anion-radical by about half its length, and the stacks from the layers

separated with cations have different tilt angles of cation-radicals (Fig. 4).

Based on chemical formula **1**, one can conclude that the averaged value of the charge on TCNQ^{-q} particles is -0.5 and -1.0 per two TCNQ formula units. Taking into account the presence of two crystallographically non-equivalent TCNQ particles in the ARS **1** structure, the charges on them can be estimated
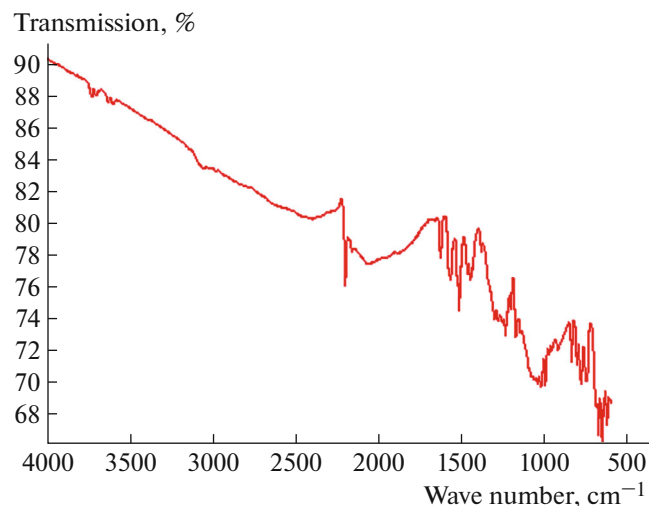

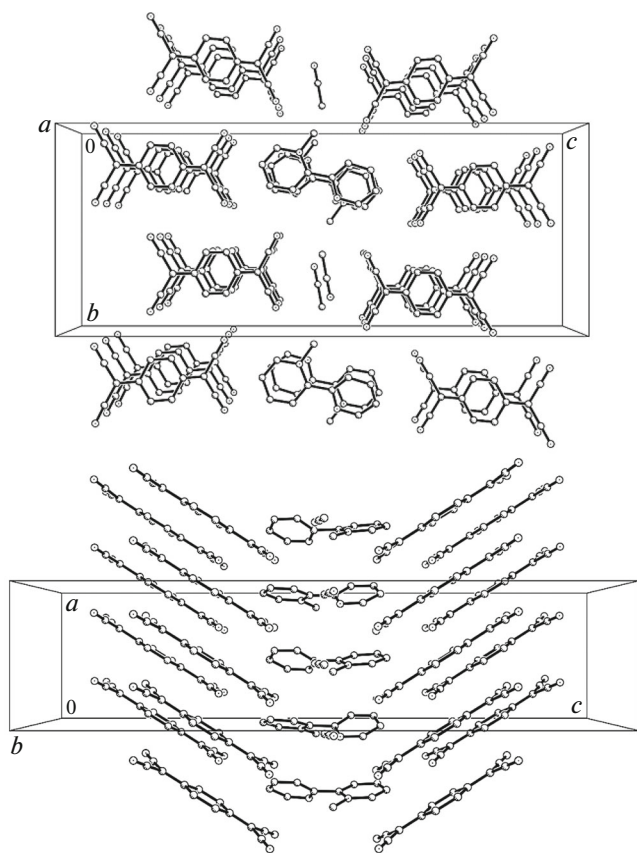**Fig. 2.** IR spectrum of ARS **1**.

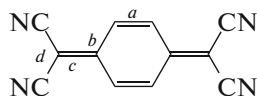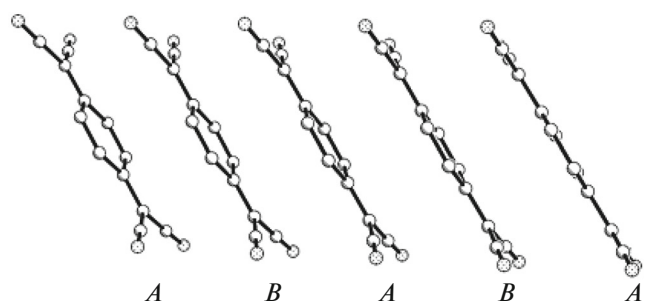**Fig. 3.** Fragments of the crystal structure of ARS **1** (hydrogen atoms are omitted).

Fig. 4. Alternation of anion-radicals in stack **1** (hydrogen atoms are omitted).

symmetrical vibrations against its background (these lines are forbidden in the IR spectrum in the absence of this interaction).

As can be seen in Fig. 2, there is continuous absorption in the spectrum of ARS **1** in the entire range of wavenumbers under study, and the lines in the ranges of $900-1400$ and $1800-2100$ cm^{-1} are strongly broadened. These features, being characteristic of high-conductivity TCNQ ARSs, are due to the electron–phonon interaction [1, 2]. This interaction causes "build-up" of the totally symmetric vibrations of TCNQ (forbidden by the selection rules) and their significant broadening. They manifest themselves against the electron-continuum background, the beginning of which is determined by the band gap. This fact suggests that the ARS under consideration is an organic metal or a narrow-gap semiconductor. The band gap is limited by the following relation [2]:

$$\Delta \leq h\nu_0,$$

where Δ is the band gap and ν_0 is the continuous-absorption beginning. In this case, we have the following estimate: $\Delta \leq 0.07$ eV.

based on the following relation (proposed by Kistenmacher):

$$q = -41.67[c/(b + d)] + 19.83,$$

where the parameters c, b, and d are the corresponding bond lengths (Scheme 1) [14, 15].

Using the data of Table 1, one can find that two types of TCNQ particles have charges of -0.55 and -0.32. Taking into account the approximate character of the method in use, these values can be considered as satisfactory; there is a weak alternation of the charge of TCNQ particles in the ARS crystals.

It is known [1, 2] that the IR spectrum of conducting TCNQ ARSs have some specific features related to the electron–phonon interactions. In particular, one can observe continuous absorption, the beginning of which corresponds to the band gap, and lines of totally

CONCLUSIONS

The synthesized ARS contains isolated stacks of TCNQ anion-radicals with a weak charge alternation. The ARS structure favors the formation of the conducting state of the salt, which was confirmed by its IR spectrum: the continuous absorption spectrum gives grounds to assign this ARS to organic metals or narrow-gap semiconductors (the band gap does not exceed 0.07 eV).

REFERENCES

1. V. A. Starodub and T. N. Starodub, Russ. Chem. Rev. **83** (5), 391 (2014).
   https://doi.org/10.1070/RC2014v083n05ABEH004299

2. V. A. Starodub, T. N. Starodub, O. N. Kazheva, and V. I. Bregadze, *Materials of Modern Electronics and Spintronics* (Fizmatlit, Moscow) [in Russian], 424 (2018).

Scheme 1. Parameters used in the Kistenmacher formula.

3. K. Ueda, T. Sugimoto, S. Endo, et al., Chem. Phys. Lett. **261**, 295 (1996). https://doi.org/10.1016/0009-2614(96)00982-7

4. T. Sugimoto, K. Ueda, M. Tsujii, et al., Chem. Phys. Lett. **249**, 304 (1996). https://doi.org/10.1016/0009-2614(95)01418-7

5. D. V. Ziolkovsky, A. V. Kravchenko, V. A. Starodub, et al., Funct. Mater. **12**, 577 (2005).

6. D. V. Ziolkovskiy, O. N. Kazheva, G. V. Shilov, et al., Funct. Mater. **13**, 119 (2006).

7. B. Barszcz, A. Graja, D. V. Ziolkovskiy, and V. A. Starodub, Synth. Met. **158**, 246 (2008). https://doi.org/10.1016/j.synthmet.2008.01.010

8. A. Radvakova, D. V. Ziolkovskiy, V. O. Cheranovskii, et al., J. Phys. Chem. Solids **70**, 1471 (2009). https://doi.org/10.1016/j.jpcs.2009.09.004

9. A. Piotrowska, J. Drzeżdżon, D. Jacewicz, and L. Chmurzyński, Wiadomości Chem. **71**, 220 (2017). http://www.dbc.wroc.pl/dlibra/docmetadata?id=36712&from=publication.

10. M. Tichoniuk, M. Ligaj, and M. Filipiak, Sensors **8**, 2118 (2008). https://doi.org/10.3390/s8042118

11. V. A. Starodub, E. M. Gluzman, Yu. A. Kaftanova, and J. Olejniczak, Theor. Exp. Chem. **33** (2), 95 (1997). https://doi.org/10.1007/BF02765953

12. O. V. Dolomanov, L. J. Bourhis, R. J. Gildea, et al., J. Appl. Crystallogr. **42**, 339 (2009). https://doi.org/10.1107/S0021889808042726

13. G. M. Sheldrick, Acta Crystallogr. A **71**, 3 (2015). https://doi.org/10.1107/S2053273314026370

14. Ö. Üngör, H. Phan, E. Sang Choi, et al., J. Magn. Magn. Mater. **497**, 165984 (2020). https://doi.org/10.1016/j.jmmm.2019.165984

15. Th. J. Kistenmacher, Th. J. Emge, A. N. Bloch, and D. O. Cowan, Acta Crystallogr. B **38**, 1193 (1982). https://doi.org/10.1107/S0567740882005275

Translated by Yu. Sin'kov